X-ray photoemission and Auger-electron spectroscopic study of the electronic structure of intercalation compounds $M_x TiS_2$ (M = Mn, Fe, Co, and Ni)

A. Fujimori*
National Institute for Research in Inorganic Materials, Tsukuba, Ibaraki 305, Japan

S. Suga
Synchrotron Radiation Laboratory, Institute for Solid State Physics, The University of Tokyo, Tanashi, Tokyo 188, Japan

H. Negishi and M. Inoue
Department of Materials Science, Faculty of Science, Hiroshima University, Hiroshima 730, Japan
(Received 22 December 1987; revised manuscript received 15 March 1988)

The electronic structure of intercalation compounds $M_x TiS_2$ (M = Mn, Fe, Co, and Ni) has been studied by x-ray photoemission spectroscopy (XPS) and Auger-electron spectroscopy. The intercalated M $3d$-derived spectra in the valence-band region can be interpreted in terms of multiplet and satellite structures, suggesting that the intra-atomic Coulomb and exchange energies for the M $3d$ electrons and the M $3d$-S $3p$ hybridization dominate the M $3d$-band width. The core-level XPS spectra of the guest $3d$ atoms also exhibit multiplet and satellite structures, from which these atoms are found to be in high-spin divalent states, except for Co, which is in the low-spin divalent state. The host Ti $3d$- and S $3p$-derived electronic states, on the other hand, are basically well described by the band theory. Auger-electron spectra also support the strong electron correlation of the M $3d$ states and its insignificance for the host Ti $3d$ and S $3p$ states. Itinerant behaviors of the M $3d$ electrons as observed in the magnetic, thermal, and transport properties combined with the present results suggest that correlated M $3d$ bands are formed in these compounds as a result of strong hybridization with the host electronic states. The Ti $2p$ core-level XPS spectra of $M_x TiS_2$ are shown to consist of poorly screened and well-screened peaks. As for TiS_2, the Ti $2p$ XPS spectrum does not show well-screened peaks because of the absence of conduction electrons that can fill the screening orbital, whereas this orbital appears to be filled in the initial state of Auger-electron emission.

I. INTRODUCTION

$3d$ transition-metal atoms (M) can be intercalated into the van der Waals gaps of layered-structure transition-metal dichalcogenides TX_2, where T and X stand, respectively, for a transition metal and a chalcogen atom. The physical properties of compounds $M_x TX_2$ thus formed are considerably modified from those of the host materials.[1,2] The electronic and magnetic properties of $M_x NbS_2$, $M_x TaS_2$, and $M_x NbSe_2$ have been understood in terms of a rigid-band model,[2-5] according to which the guest $3d$ atoms donate electrons to the partially filled d_{z^2} band of the host material and become divalent or trivalent ions. The $3d$ electrons of the guest atoms are localized and interact with each other via Ti $3d$ conduction electrons through Ruderman-Kittel-Kasuya-Yosida (RKKY) interaction,[6] resulting in various types of magnetic orderings; the anomalous transport properties are explained as due to scattering of conduction electrons by the local spins.[5]

Recent detailed studies on $M_x TiS_2$ (M = V, Cr, Mn, Fe, Co, and Ni),[7-9] however, have revealed itinerant behaviors of the intercalated M $3d$ electrons as follows: (i) The magnitude of the ordered moment is generally smaller than those expected from the above rigid-band model, particularly for $Co_x TiS_2$;[7] (ii) The electronic specific-heat coefficient γ is unusually large (e.g., $\gamma \simeq 80$ mJ, $mol^{-1} K^{-2}$ for $M_{1/4} TiS_2$),[8] suggesting significant M $3d$ contributions at the Fermi level (E_F); (iii) the appearance of hole pockets in $Ni_x TiS_2$ suggested from Hall measurements[9] cannot be explained by the rigid-band model and imply a strong modification of the band structure by the intercalated Ni $3d$ states. Yamasaki, Suzuki and Motizuki[10] and Suzuki *et al.*[11] have made band-structure calculations on $Cr_x TiS_2$ and $Fe_x TiS_2$ in paramagnetic and ferromagnetic states using the augmented-plane-wave (APW) method. Their results have indicated a strong hybridization between the host Ti $3d$-S $3p$ states and the intercalated M $3d$ states. They have thus concluded that the itinerant-band model rather than the rigid-band model is appropriate to describe the electronic structure of $M_x TiS_2$. Recently Ueda *et al.*[12,13] have performed ultraviolet-photoemission-spectroscopy (UPS) measurements on $M_x TiS_2$ using synchrotron radiation in the photon-energy range $h\nu = 32-120$ eV in order to study experimentally their electronic structures. By using the resonant photoemission technique, they have demonstrated the strong hybridization between the guest $3d$ and the host electronic states.

Since UPS is a rather surface-sensitive technique, it

probes electronic states in the surface region which may be modified from those in the bulk. Thus we have performed x-ray-photoemission-spectroscopy (XPS) measurements which are more bulk sensitive due to the longer photoelectron mean free paths. In this paper, we present the results of the XPS studies as well as those of Auger-electron-spectroscopy studies on $M_X TiS_2$ ($x=\frac{1}{3}$ or $\frac{1}{4}$, M=Mn, Fe, Co, and Ni), where the guest $3d$ atoms form $\sqrt{3}\times\sqrt{3}$ and 2×2 superlattices for $x=\frac{1}{3}$ and $\frac{1}{4}$, respectively, as shown in Fig. 1. The spectra are compared with band theory[10,11] and configuration-interaction (CI) theory in order to evaluate the degree of hybridization between the host and guest electronic states and also the magnitude of the intra-atomic Coulomb energy for the M $3d$ electrons which play crucial roles in determining the itinerant versus localized behaviors of these electrons. Our results have confirmed the strong hybridization between the M $3d$ and S $3p$ states as suggested by the band-structure calculations[10,11] and by the synchrotron-radiation photoemission studies.[12,13] Furthermore, we have found that the intra-atomic Coulomb energy between the M $3d$ electrons is generally large and dominates the one-electron M $3d$-band width, whereas electron correlation is not important for the host Ti $3d$- and S $3p$-derived states. It is thus proposed that the itinerant behaviors of the M $3d$ electrons should be ascribed to those of correlated energy bands resulting from the hybridization between the bandlike host Ti $3d$ and S $3p$ states and the atomiclike M $3d$ states. These conclusions will be derived from analyses of the core-level XPS spectra of the guest $3d$ atoms (Sec. III A), S and Ti (Sec. III B), the valence-band XPS spectra (Sec. III C), and the Auger-electron spectra (Sec. III D).

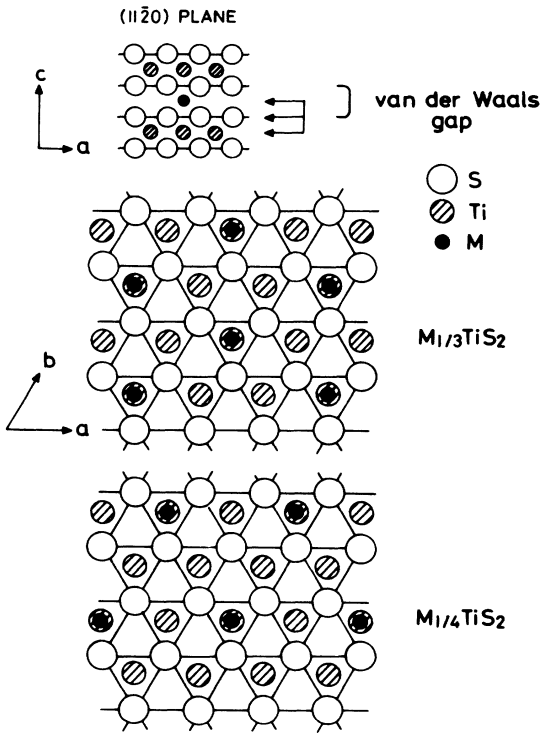

FIG. 1. Crystal structures of $M_{1/3}TiS_2$ and $M_{1/4}TiS_2$. The three layers indicated by arrows are shown in the bottom two panels.

II. EXPERIMENT

Single crystals of $M_x TiS_2$ were grown by a chemical-vapor-transport technique using iodine as a carrier gas as described elsewhere.[14] XPS and Auger measurements were made by using a spectrometer equipped with a Mg x-ray source and a double-pass cylindrical-mirror analyzer (PHI model 15-255). The samples were glued onto sample holders using conductive epoxy. Clean surfaces were obtained by scraping with a diamond file in the spectrometer chamber having a base pressure of $\sim1\times10^{-10}$ Torr. The cleanliness of the surface was checked through the absence or weakness of the O $1s$ XPS signal. The spectra have been corrected for the Mg $K\alpha_{3,4}$ satellite and for the kinetic-energy dependence of the analyzer transmission efficiency.[15] The resolution of the electron-energy analyzer was 0.6–0.8 eV depending on the pass energy and the aperture size[15] and a total resolution of about 1 eV was obtained combined with the natural width of the x rays. Experimental errors in binding energies (E_B) were ±0.1 eV.

III. RESULTS AND DISCUSSION

A. Core levels of guest $3d$ transition metals

Core-level XPS spectra of $3d$ transition-metal oxides, halides, and chalcogenides exhibit satellite structures: Each metal core-level spectrum consists of the "main peak" and the "satellite" at lower (smaller) and higher (larger) binding energies, respectively. It is now established that except for early $3d$ transition-metal (Sc, Ti, and V) compounds,[16] the main peak usually corresponds to final states with the core hole screened by ligand-to-metal charge transfer (i.e., $\underline{c}d^{n+1}\underline{L}$ final states, where $\underline{c}$ and $\underline{L}$ denote a core hole and a ligand hole), and that the satellite corresponds to final states with an unscreened core hole ($\underline{c}d^n$ final states).[17] The M $2p$ core-level spectra for $M_x TiS_2$ are collected in Fig. 2. In the figure one can see that each of the spin-orbit components, $2p_{3/2}$ and $2p_{1/2}$, indeed shows a satellite feature, except for the Co $2p$ spectrum, for which the satellite is not so well defined as in the other M $2p$ spectra.

In Figs. 3–5 the M $2p$ spectra are compared with those of some $3d$ transition-metal sulfides. In Fig. 3 the Fe $2p$ spectrum of $Fe_{1/3}TiS_2$ is compared with those of two representative divalent Fe sulfides, FeS_2 (Ref. 18) and hexagonal FeS (Ref. 19), in which Fe is in the low-spin ($S=0$) and high-spin ($S=2$) states, respectively. There one can clearly see that the Fe $2p$ spectrum of $Fe_{1/3}TiS_2$ is rather similar to that of FeS concerning the peak positions and the satellite line shape than to that of FeS_2. The great similarity between the spectra of $Fe_{1/3}TiS_2$ and FeS is consistent with the fact that Fe in $Fe_{1/3}TiS_2$ has been found to be in the high-spin divalent state by the ^{57}Fe Mössbauer studies.[7] Since the satellite structures reflect the degree of hybridization between the $3d$ and

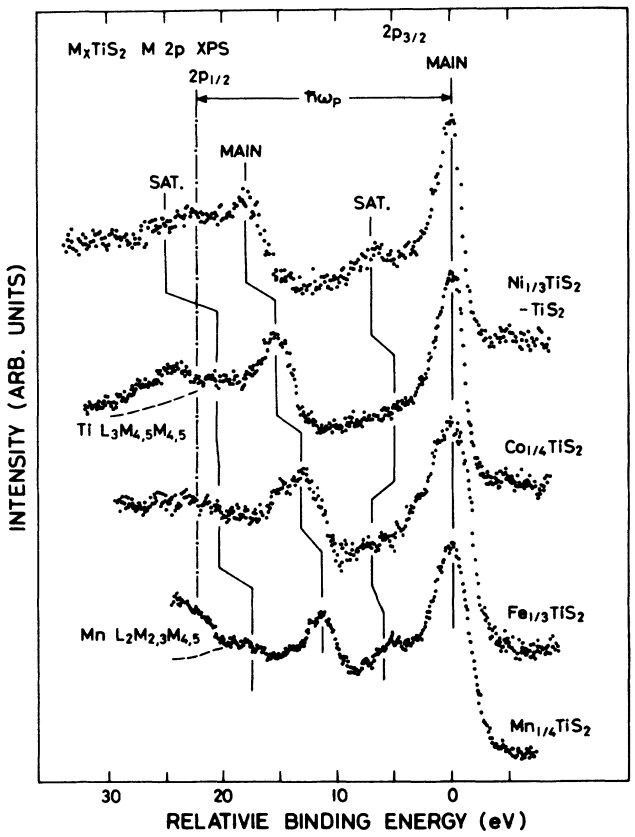

FIG. 2. 2p core-level XPS spectra of guest 3d-transition-metal atoms in M_xTiS_2. The $2p_{3/2}$ peaks of different compounds have been aligned. $\hbar\omega_p$ marks approximately the bulk-plasmon energy obtained from the energy position of the plasmon satellite accompanying the S 2p core-level XPS peak.

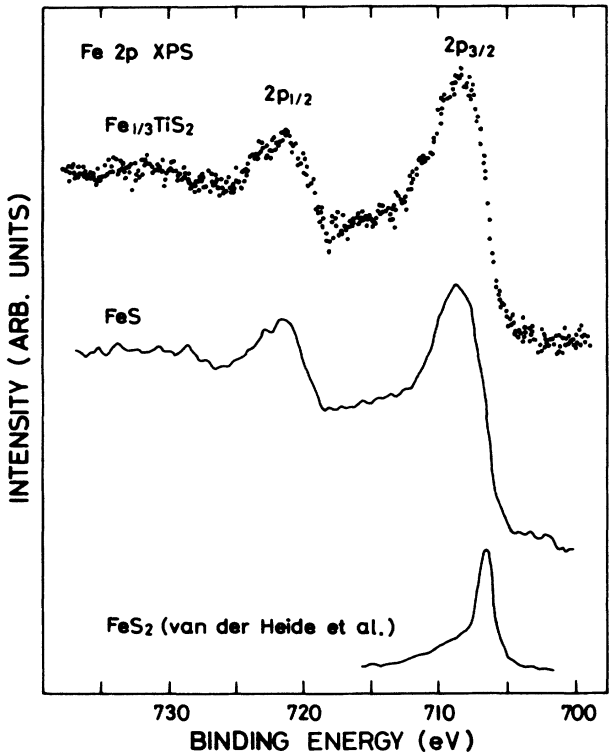

FIG. 3. Fe 2p core-level XPS spectrum of $Fe_{1/3}TiS_2$ compared with those of the low-spin FeS_2 (Ref. 18) and the high-spin FeS (Ref. 19).

ligand orbitals, we may conclude that the Fe 3d–S 3p hybridization strengths are similar in Fe_xTiS_2 and FeS. Such a similarity is expected as the local environment of the Fe atom is similar between the two systems, in that the Fe atom is octahedrally coordinated by six S atoms which form hexagonal-close-packed structures. (The Fe atom in FeS_2 is coordinated by six S_2^{2-} molecules and the Fe 3d electrons are in the low-spin state.)

Figure 4 shows the results for $Ni_{1/3}TiS_2$, where the Ti $L_3M_{2,3}M_{2,3}$ Auger emission which overlaps the Ni 2p region has been subtracted using the spectrum of TiS_2. As shown in Fig. 4, the peak position and the satellite line shape of the Ni 2p core-level XPS spectrum of $Ni_{1/3}TiS_2$ is quite similar to that of hexagonal NiS,[20] in which Ni is in the high-spin ($S=1$) divalent state.[21] In Fig. 5 the Co 2p spectrum of $Co_{1/4}TiS_2$ is compared with that of the low-spin ($S=\frac{1}{2}$) pyrite-type CoS_2 (Ref. 18) and that of hexagonal CoS,[22] which is intermediate between the low-spin and high-spin states.[23] The spectrum of $Co_{1/4}TiS_2$ is closer to that of CoS_2, in that the sattelite is weak and does not exhibit a well-defined peak or a shoulder. The satellite structure of the Mn 2p core level is similar to that of MnS_2,[18] consistent with the high-spin, divalent Mn atom.

The valence and spin states of the guest 3d atoms can also be studied through the exchange splittings of the M 3s core levels. The 3s core-level spectra of M_xTiS_2 are shown in Fig. 6, where the spectra are compared with the exchange-split multiplets (intensities are given by the height of the bars) expected for the $\underline{3s}3d^n$ and $\underline{3s}3d^{n+1}$ configurations for the satellites and the main peaks, respectively, where n is the nominal d occupation in the ground state, i.e., $n=5$, 6, 7, and 8 for $M=$Mn, Fe, Co, and Ni. The exchange splitting, namely the energy separation between the two components in each multiplet, has been taken to be equal to that of the main 3s peak in 3d transition-metal difluorides.[24] (We attribute the main peaks in the fluorides to unscreened $\underline{3s}3d^n$ final states rather than to screened $\underline{3s}3d^{n+1}\underline{L}$, in contrast to what was suggested by Veal and Paulikas.[25] This is because the F 2p valence band lies deep, i.e., $\sim$10 eV below E_F,[26] and consequently it would cost energy to transfer an electron from the F 2p band to the 3d state.) The intensity ratio between the exchange-split components has been taken to be proportional to the final-state spin multiplicity with a modification that the intensity of the high-binding-energy component is multiplied by 0.64 according to Fadley *et al.*[27] The separation between the satellite ($\underline{3s}3d^n$) and main-peak ($\underline{3s}3d^{n+1}\underline{L}$) multiplets for each material has been taken to be 80% of that of the 2p core-level spectrum (corresponding to the weaker core-hole potential of the relatively extended 3s orbital than that of

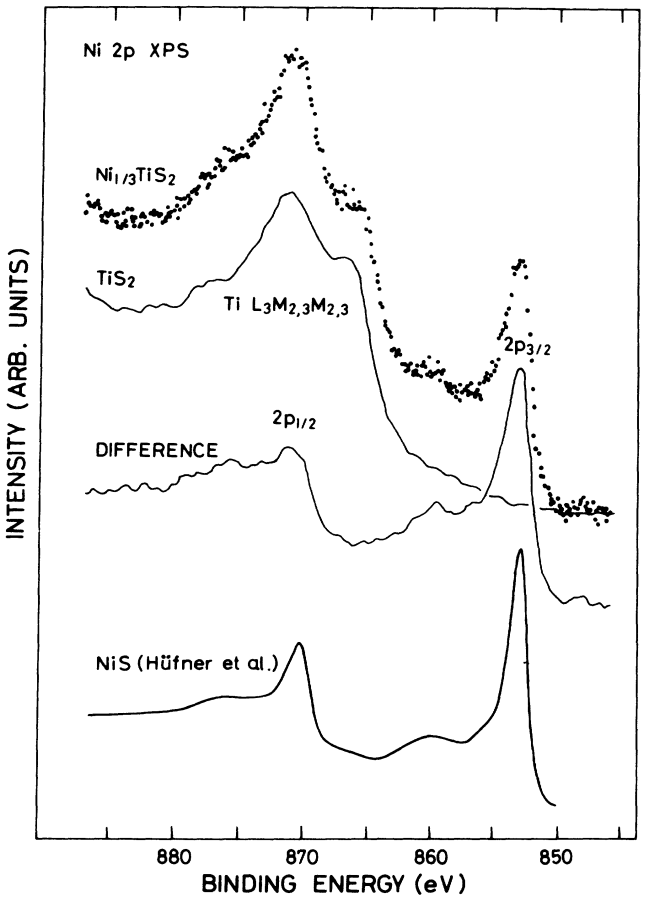

FIG. 4. Ni $2p$ core-level XPS spectrum of $Ni_{1/3}TiS_2$ compared with that of NiS (Ref. 20). The overlapping Ti $L_3M_{2,3}M_{2,3}$ Auger emission has been eliminated by subtracting the spectrum of TiS_2.

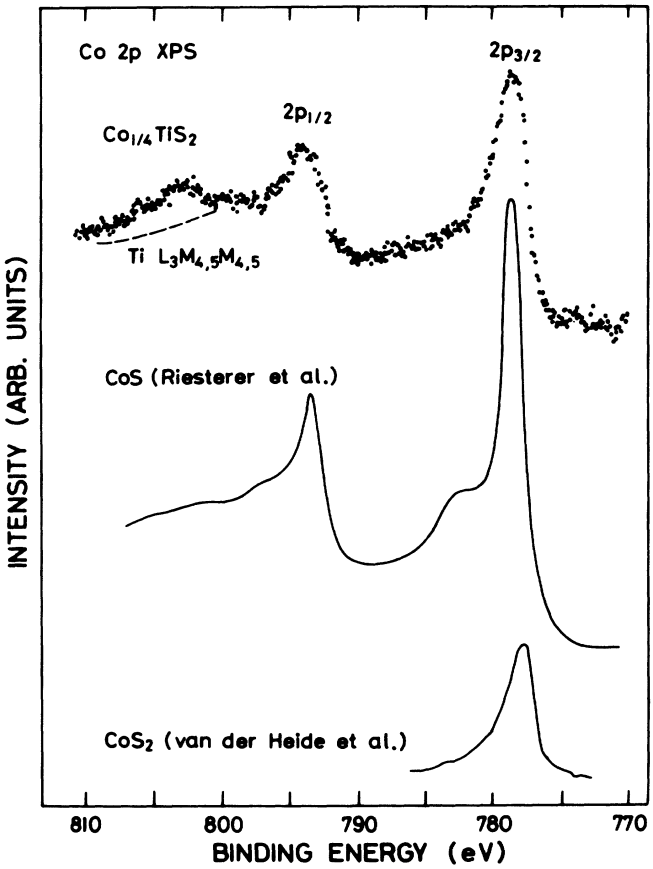

FIG. 5. Co $2p$ core-level XPS spectrum of $Co_{1/4}TiS_2$ compared with those of CoS_2 (Ref. 18) and CoS (Ref. 22).

the $2p$ orbital). The calculated bar diagrams thus obtained explain the experimental results within the limited experimental resolution and signal-to-noise ratios, consistent with the M $2p$ results. (As for $Co_{1/4}TiS_2$, both up-spin and down-spin unoccupied orbitals exist on the low-spin Co atom, and therefore an electron can be transferred to either orbital in the charge-transfer screening process; thus the Co $3s$ main peak in Fig. 6 is compared with the bar diagram consisting of $S=0$ and $S=1$ $3d^8$ valence configurations, corresponding to the central bar and the remaining two bars, respectively.)

The appearance of multiplet and satellite structures generally imply that the Coulomb and exchange interaction between the core hole and valence electrons is comparable to or larger than the one-electron band width of the local density of states (DOS) at the core-hole site. As the intra-atomic Coulomb interaction between the M $3d$ electrons is not expected to be much weaker than that between the core hole and $3d$ electrons and as the exchange interaction is even stronger among the $3d$ electrons, the above core-level results suggest that electron correlation between the intercalated $3d$ electrons is important and cannot be neglected in understanding the electronic structure of M_xTiS_2.

B. Core level of Ti and S

In contrast to the core-level XPS spectra of the guest $3d$ atoms, the XPS spectra of S core levels do not show multiplet nor charge-transfer satellite structures. The spectra could be fitted by simple theoretical curves, namely, spin-orbit doublets where each peak has a Lorentzian- and Gaussian-broadened asymmetric line shape given by Doniach and Šunjić [28] or by Mahan.[29]

Figure 7 shows the S $2p$ core-level spectra of M_xTiS_2 and TiS_2, which have been fitted to a single spin-orbit doublet with the statistical branching ratio of 2:1 for the $2p_{3/2}$ and $2p_{1/2}$ components. Fitted parameters such as singularity indices α, Lorentzian full widths at half maximum (FWHM), 2γ, and Gaussian FWHM, $2G$, are given in Table I.[30] The singularity index is finite ($\alpha=0.11$) for TiS_2, and increases with guest-atom concentration, consistent with an increase in the density of states (DOS) at E_F,[31] since α in metallic systems is known to be proportional to the square of the local DOS at E_F on the core-hole site.[32] We also find that the S $2p$ core-level binding energy increases with gues-atom concentration as shown in Fig. 7 or in Table I, qualitatively consistent with a shift in E_F due to the filling of the Ti $3d$ band. Apart from the

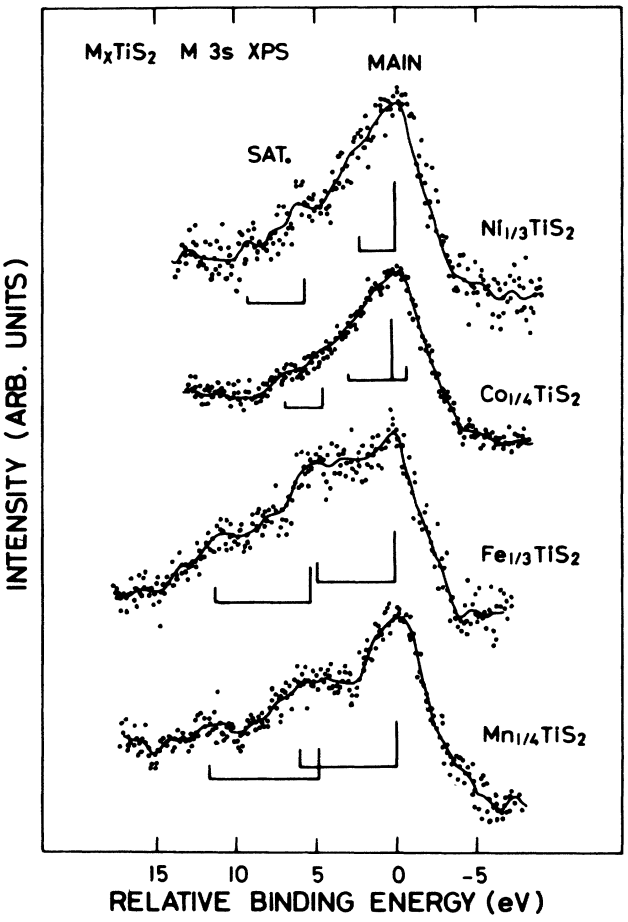

FIG. 6. 3*s* core-level XPS spectra of guest 3*d*-transition-metal atoms in M_XTiS_2. The bar diagrams show the multiplet structures of the $\underline{3s}3d^n$ and $\underline{3s}3d^{n+1}$ configurations for the satellite and the main peak, respectively. For the Mn 3*s* spectrum, a plasmon satellite at about −6 eV accompanying the Ti 3*s* core-level peak has been subtracted.

TABLE I. Line-shape parameters for the S 2*p* core-level XPS spectra of TiS_2 and M_xTiS_2. $E_B(2p_{3/2})$ is the S $2p_{3/2}$ core-level binding energy, α is the singularity index, and $2G$ is the Gaussian FWHM. The Lorentzian FWHM and the $2p_{3/2}$-$2p_{1/2}$ spin-orbit splitting have been assumed to be the same as those of TiS_2: $2\gamma = 0.54$ eV and $\Delta E_{so} = 1.16$ eV. Energies are in eV.

	$E_B(2p_{3/2})$	α	$2G$
TiS_2	160.9	0.11	0.82
$Mn_{1/4}TiS_2$	161.1	0.16	0.91
$Fe_{1/3}TiS_2$	161.2	0.22	0.90
$Co_{1/4}TiS_2$	161.0	0.16	0.90
$Ni_{1/3}TiS_2$	161.1	0.19	0.76[a]

[a]Spectra for $Ni_{1/3}TiS_2$ have been taken with higher resolution, so that this $2G$ value cannot be directly compared with those of the other compounds.

effect of the band filling, one would expect that a formation of additional bonding between the guest 3*d* and host *S* atoms causes the S 2*p* core-level shift to lower binding energies, as the bonding is expected to be partially ionic. Such an effect, however, could not be identified probably because the effect is small as compared to the shifts due to the band filling.

The Ti 2*p* core-level XPS spectra shown in Fig. 8 exhibit much more pronounced broadening and binding-energy shifts on going from TiS_2 to the intercalated compounds than in the case of the S 2*p* spectra. In particular, we note that the shift is in the opposite direction to that expected from the band-filling effect. We first made line-shape analyses using a single spin-orbit doublet and ob-

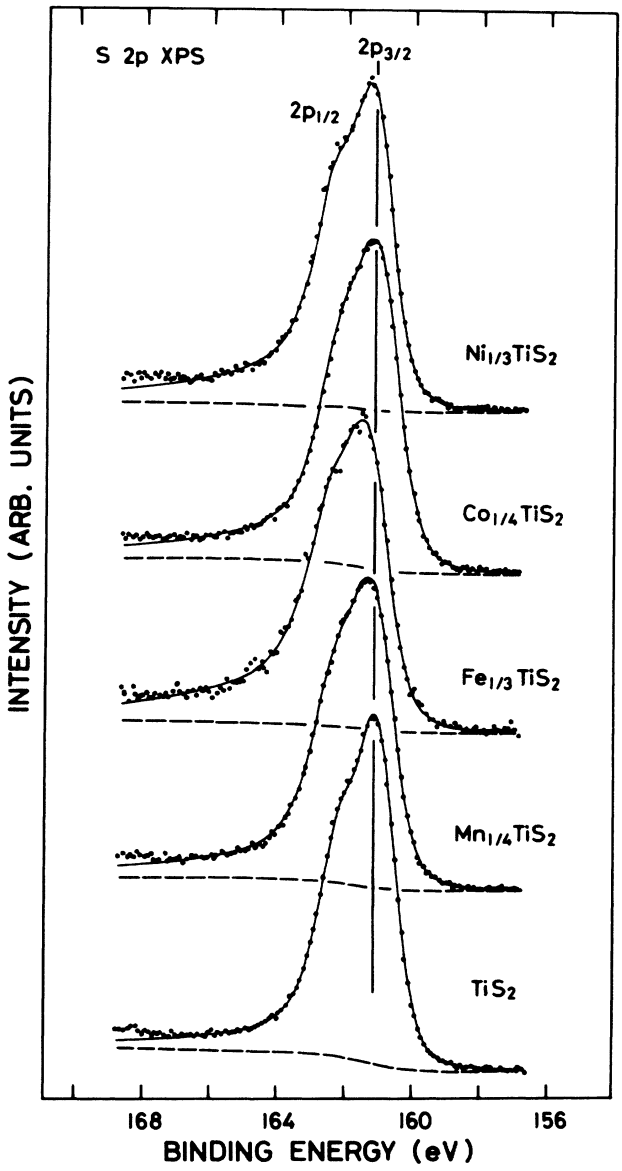

FIG. 7. S 2*p* core-level XPS spectra of TiS_2 and M_xTiS_2. The experimental spectra (dots) are fitted to theoretical curves (solid curves) calculated by using the parameters listed in Table I. The dashed curves represent integral backgrounds. The vertical line marks the peak position for TiS_2.

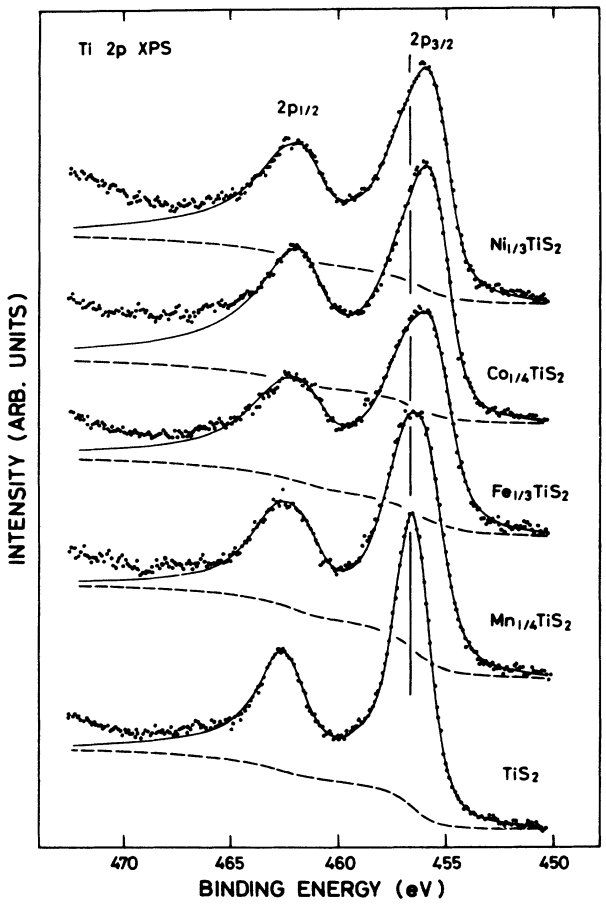

FIG. 8. Ti $2p$ core-level XPS spectra of TiS_2 and M_xTiS_2. The experimental spectra (dots) are fitted to theoretical curves (solid curves) calculated by using the parameters listed in Table III (for TiS_2, in Table II). Except for TiS_2, each theoretical curve consists of two overlapping spin-orbit doublets as shown in Figs. 9 and 10. The vertical line marks the $2p_{3/2}$ peak position for TiS_2.

tained parameters listed in Table II.[33] The resulting fits are shown on the bottom of Figs. 9 and 10 for $Ni_{1/3}TiS_2$ and $Mn_{1/4}TiS_2$. One can notice in Table II that the Gaussian FWHM for the intercalation, $2G$, compounds are considerably larger (by 0.5–0.8 eV) than that for TiS_2. This may suggest an overlap of different components in the Ti $2p$ spectra, either due to an initial-state effect, i.e., the presence of inequivalent Ti sites, or due to a final-

TABLE II. Line-shape parameters for the Ti $2p$ core-level XPS spectra of TiS_2 and M_xTiS_2 obtained by assuming a single spin-orbit doublet. The $2p_{3/2}$-$2p_{1/2}$ spin-orbit splitting has been fixed at $\Delta E_{so}=6.01$ eV as obtained for TiS_2. Energies are in eV.

	$E_B(2p_{3/2})$	α	$2\gamma_{3/2}$	$2\gamma_{1/2}$	$2G$
TiS_2	456.4	0.16	0.93	1.74	1.03
$Mn_{1/4}TiS_2$	456.2	0.18	0.78	1.80	1.79
$Fe_{1/3}TiS_2$	455.7	0.37	0.59	1.78	1.83
$Co_{1/4}TiS_2$	455.6	0.39	0.67	1.44	1.51
$Ni_{1/3}TiS_2$	455.6	0.39	0.63	1.51	1.51

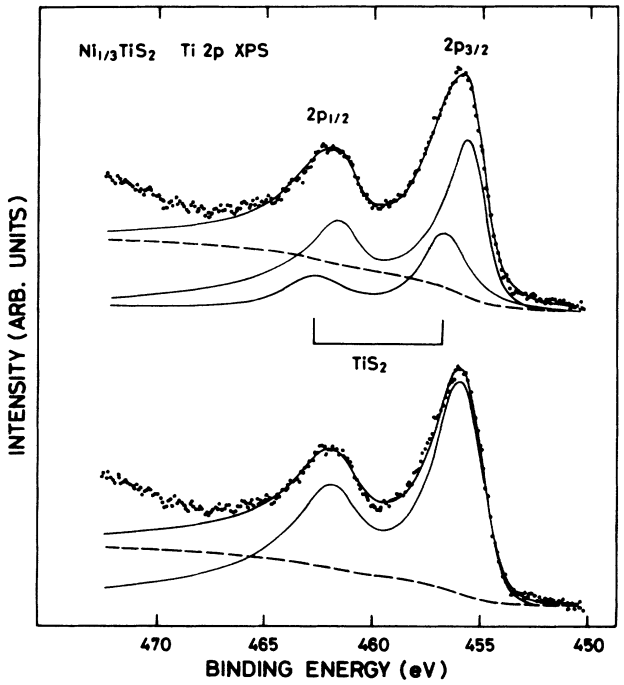

FIG. 9. Ti $2p$ core-level XPS spectrum of $Ni_{1/3}TiS_2$ fitted to a single spin-orbit doublet (bottom) and to a superposition of two spin-orbit doublets (top). Respective line-shape parameters are given in Tables II and III. The $2p_{3/2}$ and $2p_{1/2}$ peak positions for TiS_2 (corrected for the filling of the Ti $3d$ conduction band in $Ni_{1/3}TiS_2$ as described in the text) are indicated.

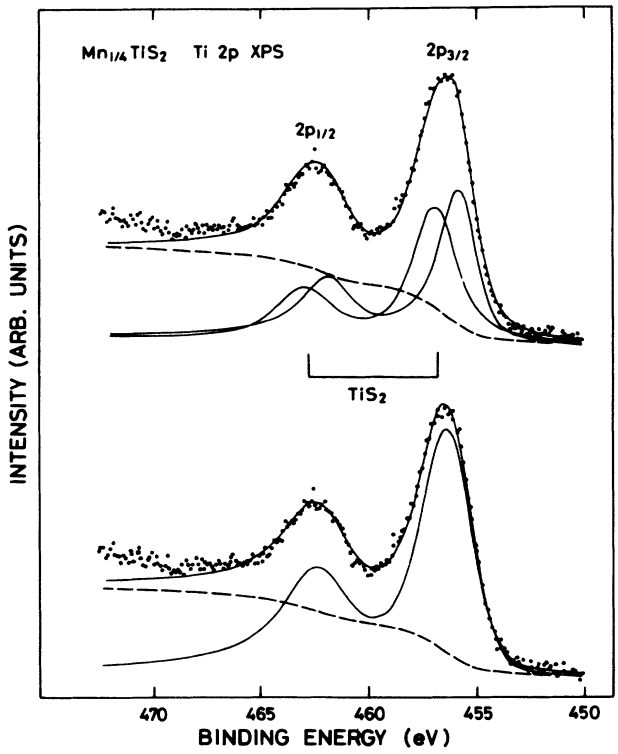

FIG. 10. Ti $2p$ core-level XPS spectrum of $Mn_{1/4}TiS_2$ fitted to a single spin-orbit doublet and to a superposition of two spin-orbit doublets. The same as Fig. 9.

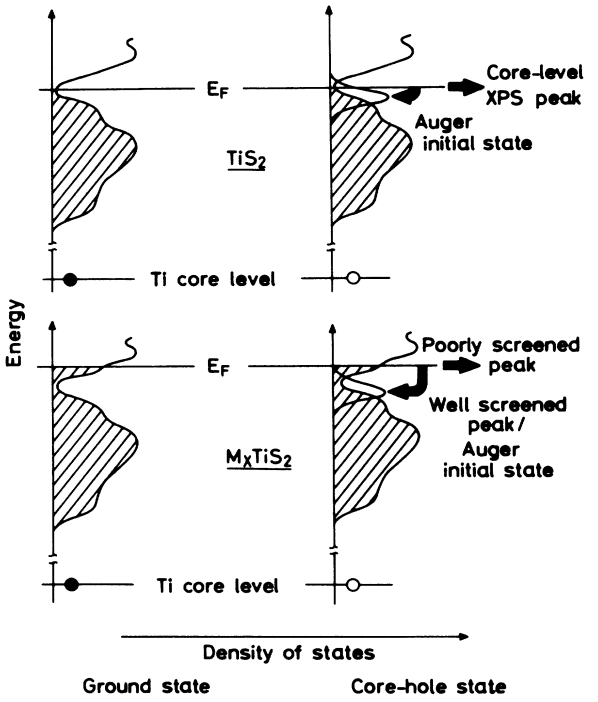

FIG. 11. Screening processes for Ti core holes in TiS_2 and M_xTiS_2. A screening level of Ti $3d$ character is formed below the Fermi level (E_F) in the core-hole state. An electron from the conduction band fills this level in the well-screened core-hole state and does not in the poorly screened core-hole state. The screening level is filled also in the initial state of Auger-electron emission. For TiS_2, the probability of filling the screening orbital is very small in the photoemission final state because of the almost empty Ti $3d$ conduction band.

state effect such as the existence of different screening channels. Indeed, the theoretical curves using a single spin-orbit doublet in Figs. 9 and 10 show misfits in the region $E_B \simeq 455-462$ eV. A possible initial-state effect is an overlap of Ti^{4+} ($3d^0$) and Ti^{3+} ($3d^1$) components since the number of conduction electrons in the Ti $3d$ band per Ti atom ($=2x$) is less than unity for M_xTiS_2 with $x=\frac{1}{4}$ or $\frac{1}{3}$. The apparent Ti $2p$ core-level shift to lower binding energies can then be explained as due to the growth of the overlapping $\underline{2p}3d^1$ component on the low-binding-energy side of the $\underline{2p}3d^0$ component. However, Ti $3d$ electrons in M_xTiS_2 are known to behave as itinerant electrons[7-9] rather than localized ones hopping between Ti sites because of the large Ti $3d$-band width. (The nonbonding and the total Ti $3d$-conduction-band widths have been calculated to be about 2 and 3.5 eV, respectively.[10]) Thus the two components cannot be due to the presence of the two distinct initial states $3d^0$ and $3d^1$.

Then we consider a final-state effect induced by the core-hole potential as originally proposed by Kotani and Toyozawa.[34] Namely, as schematically shown in Fig. 11, the core-hole potential pulls down a localized screening level of Ti $3d$ character below E_F, which is either occupied by an electron transferred from the conduction band or unoccupied in the final state, giving rise to two components in the core-level XPS spectrum. Thus the Ti $2p$ spectra of M_xTiS_2 were fitted to a superposition of two spin-orbit doublets corresponding to a well-screened peak and a poorly screened peak appearing at lower and higher binding energies, respectively. The results of the fitting are shown in Figs. 8–10, and the parameters thus deduced are listed in Table III.[35] (The solid curves in Fig. 8, except for TiS_2, show the results of the two-component fits.) We see in Figs. 9 and 10 that the fits are significantly improved as compared to the one-component fits.

We note in Table III that the lifetime width of the poorly screened peak increases with guest-atom concentration. This can be understood if we consider the decay process of the poorly screened core-hole state into the well-screened state by filling the screening level via an Auger-type transition leaving two holes in the Ti $3d$ conduction band. The probability of this transition will increase with the number of Ti $3d$ conduction electrons supplied by the guest atoms.

For the Ti $2p$ XPS spectrum of TiS_2, although the screening level may be formed on the core-hole site, well-screened peaks are expected to be weak, because the Ti $3d$ conduction band is almost empty in TiS_2 and electron transfer from the conduction band to the screening level cannot occur effectively when the core hole is created suddenly. Indeed, the Ti $2p$ XPS peak energies for TiS_2 are found to be close to those of the poorly screened

TABLE III. Line-shape parameters for the Ti $2p$ core-level XPS spectra of M_xTiS_2 obtained by assuming two overlapping spin-orbit doublets representing well-screened and poorly screened peaks. The Gaussian FWHM and the $2p_{3/2}$-$2p_{1/2}$ spin-orbit splitting have been fixed at $2G=1.03$ eV (0.83 eV for $Ni_{1/3}TiS_2$ because of the better instrumental resolution) and $\Delta E_{so}=6.01$ eV. Energies are in eV.

	Well screened[a]			Poorly screened[b]		
	$E_B(2p_{3/2})$	α	$2\gamma_{1/2}$	$E_B(2p_{3/2})$	$2\gamma_{3/2}$	I_{PS}/I_{WS}[c]
$Mn_{1/4}TiS_2$	455.8	0.19	1.72	457.0	1.79	0.90
$Fe_{1/3}TiS_2$	455.4	0.37	1.70	456.9	2.29	0.45
$Co_{1/4}TiS_2$	455.5	0.38	1.53	457.0	1.92	0.18
$Ni_{1/3}TiS_2$	455.3	0.39	1.62	456.7	2.24	0.37

[a] $2\gamma_{3/2}$ has been fixed at 0.93 eV.

[b] α has been fixed at zero. We have assumed $2\gamma_{1/2}-2\gamma_{3/2}$ to be the same as that for the well-screened peaks.

[c] Intensity ratios between the poorly screened (PS) and well-screened (WS) peaks.

peaks for M_xTiS_2 (Tables II and III, Figs. 9 and 10) and no trace of well-screened peaks is observed in the TiS_2 spectrum (Fig. 8). [In Figs. 9 and 10, the Ti $2p$ peak positions for TiS_2 have been shifted to higher binding energies relative to those of M_xTiS_2 by the same amount as the S $2p$ shift (0.1–0.3 eV) in order to take into account the band-filling effect in M_xTiS_2.] Further evidence for the formation of the screening level in TiS_2 will be given in Sec. II D based on the analysis of Auger-electron spectra.

The splitting between the well-screened and poorly screened Ti $2p$ peaks, ~ 1.5 eV, is the Coulomb energy Q between the Ti $2p$ core hole and the Ti $3d$ electron. If we assume that the intra-atomic Coulomb energy U amounts to $\sim 70\%$ of Q as in late-$3d$-transition-metal compounds,[36] U is estimated to be of order of 1 eV. This value is small as compared to the nonbonding Ti $3d$-band width ~ 2 eV and would not alter basically the one-electron itinerant-band picture for the Ti $3d$ states even when this band is partially filled by intercalation.

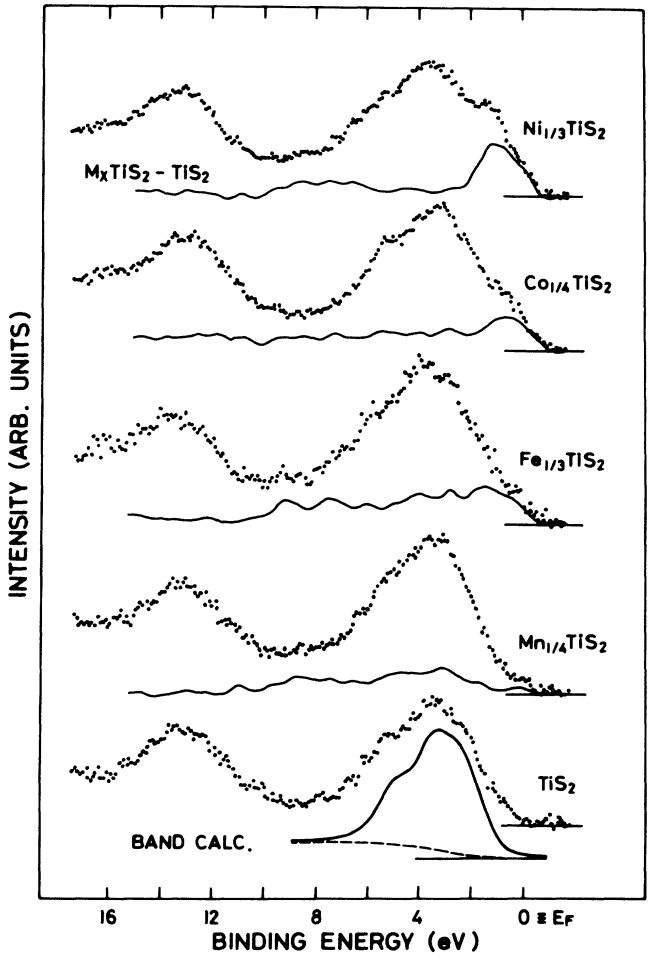

FIG. 12. XPS spectra of TiS_2 and M_xTiS_2 in the valence-band region. Difference spectra between M_xTiS_2 and TiS_2 are shown by solid curves below each of the M_xTiS_2 spectra. The TiS_2 spectrum is compared with a theoretical XPS spectrum calculated by using the energy-band density of states given by Yamasaki, Suzuki, and Motizuki (Ref. 10).

C. Valence bands

On the bottom of Fig. 12, the valence-band XPS spectrum of TiS_2 is compared with a theoretical spectrum calculated by using the DOS given by the band-structure calculation.[10] The theoretical spectrum was obtained by adding Ti $3d$ and S $3p$ partial DOS which has been multiplied by corresponding photoionization cross sections[37] and broadened with a Gaussian function ($2G=0.65$ eV) and a Lorentzian function having an energy-dependent width [$2\gamma=0.14$ eV $+0.2(E_B-E_F)$, where 0.14 eV represents the natural width of the x-ray source] in order to represent the instrumental and lifetime-broadening effects. The best agreement between theory and experiment was obtained by shifting the theoretical spectrum by 1 eV to higher binding energies, as shown in Fig. 12. Apart from this shift, correspondence between the band theory and the experimental spectrum appears satisfactory.

The valence-band XPS spectra of M_xTiS_2 are also shown in Fig. 12. These spectra and that of TiS_2 all show common characteristic features, i.e., the S $3s$ band centered at $E_B \sim 13$ eV and the S $3p$ band (the Ti $3d$–S $3p$ bonding band) within ~ 7 eV of E_F. The S $3p$ band, however, shows somewhat different line shapes for different intercalates, particularly in the region near E_F, i.e., $E_B \simeq 0$–3 eV. In order to highlight the changes induced by intercalation, the spectrum of TiS_2 was subtracted from those of M_xTiS_2 after having normalized them to the S $2p$ core-level intensity. Also, the TiS_2 spectrum was shifted so that the S $2p$ core-level peaks from TiS_2 and M_xTiS_2 were aligned, in order to take into account the effect of the band filling discussed in Sec. III B. (Without this alignment, the S $3s$ band was not canceled out, resulting in spurious structures in this region.) The difference spectra thus obtained are shown by solid curves in Fig. 12, where one can see that the difference intensities are distributed over a wide energy range, extending from E_F to $E_B \sim 10$ eV. With increasing atomic number of the $3d$ guest, the difference spectral intensity in the S $3p$-band region becomes concentrated in the low-binding-energy region $E_B \simeq 0$–3 eV. It should also be noted that every difference spectrum except for $Co_{1/4}TiS_2$ clearly shows a broad emission feature in the S $3s$-$3p$ band-gap region $E_B \simeq 6$–10 eV where no one-electron states exist.

The difference spectra represent principally contributions from the M $3d$ states. Near E_F also exist contributions from the filling of the Ti $3d$ band in M_xTiS_2. While the band-structure calculations[10,11] have shown that the intercalated M $3d$ states are strongly hybridized in the whole S $3p$-band region, the calculations cannot explain the distribution of the difference intensities in the S $3s$-$3p$ band-gap region. On the other hand, the multiplet and satellite structures of the M $3d$-photoemission final states can explain the wide distribution of the difference spectra. Indeed, in the synchrotron-radiation photoemission studies on $Ni_{1/3}TiS_2$ as a function of photon energy, the photoemission intensity at $E_B \sim 1$ eV has shown a dip, and that at $E_B \sim 6$ eV has shown a peak in the Ni $3p \rightarrow 3d$ core-excitation region, indicating that the Ni $3d$–derived

emission features at $E_B \sim 1$ eV and $E_B \sim 6$ eV correspond, respectively, to the main $3d$-band emission and the satellite.[12] In Fig. 13 the $Ni_{1/3}TiS_2$-TiS_2 difference spectrum is compared with the difference spectrum between the on- and off-resonance spectra of the Ni $3p \rightarrow 3d$ resonant photoemission for NiS, which approximately represents the Ni $3d$ partial DOS and for which the existence of the main Ni $3d$ band and the satellite has been established.[38] The overall similarity between the above two difference spectra confirms the existence of the satellite feature at $E_B \simeq 6$–10 eV in $Ni_{1/3}TiS_2$. (The relative intensities of the main band and satellite are not necessarily the same between resonant photoemission and ordinary photoemission.)

In order to obtain quantitative information about the electronic structure associated with the Ni $3d$ states from the $Ni_{1/3}TiS_2$-TiS_2 difference spectrum, configuration-interaction (CI) calculations on the NiS_6^{10-} cluster model have been performed as was previously done for NiS.[38] The cluster model assumes the ground state of the form,

$$\psi_g = a \mid d^8 \rangle + b \mid d^9 \underline{L} \rangle , \quad (1)$$

where the first term on the right-hand side represents the purely ionic configuration $Ni^{2+}(S^{2-})_6$, while the second term S-to-Ni charge-transfer states which yields covalent contributions to the ground state. The symmetry of the ground state is ${}^3A_{2g}$ (if the cluster is assumed to be cubic) corresponding to the high-spin divalent state. The charge-transfer energy $\Delta \equiv E(d^8 \rightarrow d^9 \underline{L})$, the p-d transfer integrals $(pd\sigma) \simeq -2(pd\pi)$, and the intra-atomic Coulomb energy for the Ni $3d$ electrons U were treated as adjustable parameters and were determined so as to make the calculated spectrum fit to the experimental one. The final states are given as

$$\Psi_f = a_f \mid d^7 \rangle + b_f \mid d^8 \underline{L} \rangle + c_f \mid d^9 \underline{L}^2 \rangle , \quad (2)$$

where the first term represents an unscreened Ni $3d$ hole and the remaining terms represent a $3d$ hole screened by S-to-Ni charge transfer. Our CI calculations have given an optimum fit to the experiment with the parameters $\Delta = 2.0$ eV, $(pd\pi) = -\frac{1}{2}(pd\sigma) = 0.75$ eV, and $U = 5.5$ eV as shown in Fig. 13. Considering the contributions from the partially filled Ti $3d$ conduction band near E_F in M_xTiS_2 (its approximate magnitude can be seen in Fig. 15), the agreement between theory and experiment is satisfactory.[39] The above parameter values are similar to those for NiS,[38] as would be expected from the similar S coordination of the Ni atom in both systems. The distribution of the d^7, $d^8\underline{L}$, and $d^9\underline{L}^2$ configurations in the final state is found to be such that the main band and the satellite are predominantly $d^8\underline{L}$- and d^7-like, respectively.

The final states of the Ni core-level photoemission are given by a formula similar to Eq. (2) with a similar energy-level scheme except that the Coulomb energy between the core hole and the $3d$ electron, Q, is introduced. As Q is of the same order of magnitude as U ($U \sim 0.7Q$),[36] the gross feature of the Ni $3d$-derived spectrum is expected to be similar to that of the Ni core-level spectra. Thus the presence of the satellite structure in the Ni $2p$ core-level XPS spectrum (Fig. 3) should lead to a similar satellite structure in the valence-band region. This is consistent with the assignment made in Sec. III A that the main peaks and the satellites in the Ni $2p$ XPS spectrum correspond to $\underline{2p}d^9\underline{L}$ and $\underline{2p}d^8$ final states, respectively.

The $Mn_{1/4}TiS_2$-TiS_2 difference spectrum is also compared with a CI calculation on the MnS_6^{10-} cluster model. The CI spectrum calculated with $\Delta \equiv \Delta E(d^5 \rightarrow d^6\underline{L}) = 3.5$ eV, $(pd\pi) = -\frac{1}{2}(pd\sigma) = 0.42$ eV, and $U = 7.5$ eV shown in Fig. 14 gives the best fit to the experiment. The main Mn $3d$ band at $E_B = 0$–6 eV is much broader than that of $Ni_{1/3}TiS_2$ due to the different multiplet structures. As in the case of $Ni_{1/3}TiS_2$, the main band and the satellite are predominantly $d^5\underline{L}$- and d^4-like, respectively.

CI calculations for the FeS_6^{10}-cluster in the high-spin state would be much more complicated because of CI within the d^6 configurations of the Fe^{2+} ion.[40] Instead, in Fig. 15 the $Fe_{1/3}TiS_2$-TiS_2 difference spectrum is compared with those obtained from the band-structure calculations.[10,11] For the paramagnetic state, the theory predicts a too-narrow Fe $3d$ band near E_F. As for the ferromagnetic state, the exchange splitting of the Fe $3d$ band broadens the spectrum as compared to the paramagnetic case. Still the calculated difference spectrum in the S $3p$ valence-band region $E_B = 0$–6 eV is too narrow as compared to experiment and, of course, cannot

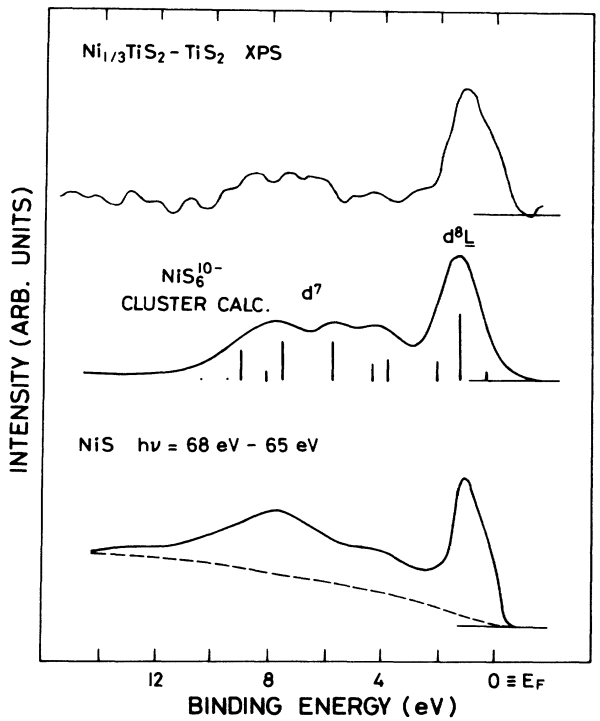

FIG. 13. Difference XPS spectrum between $Ni_{1/3}TiS_2$ and TiS_2 in the valence-band region. It is compared with a configuration-interaction calculation on the NiS_6^{-10} cluster model and with the difference between the on-resonance ($h\nu = 68$ eV) and off-resonance ($h\nu = 65$ eV) spectra of NiS in the Ni $3p \rightarrow 3d$ core-excitation region (Ref. 38).

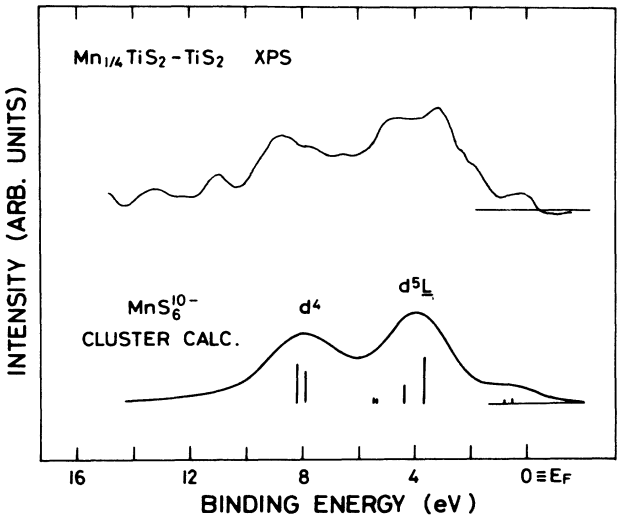

FIG. 14. Difference XPS spectrum between $Mn_{1/4}TiS_2$ and TiS_2 in the valence-band region compared with a configuration-interaction calculation on the MnS_6^{-10} cluster model. Due to the low signal-to-noise ratio, only the two peaks at $E_B \sim 4$ and 8 eV would be experimentally meaningful.

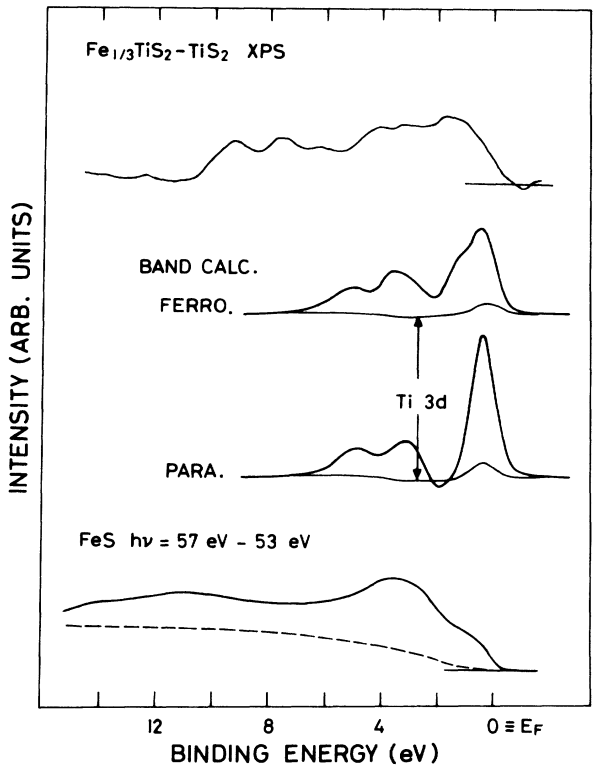

FIG. 15. Difference XPS spectrum between $Fe_{1/3}TiS_2$ and TiS_2 in the valence-band region compared with those calculated by using the energy-band densities of states of TiS_2 (Ref. 10) and of paramagnetic and ferromagnetic $Fe_{1/3}TiS_2$ (Ref. 11). It is also compared with the difference between the on-resonance ($h\nu=57$ eV) and off-resonance ($h\nu=53$ eV) spectra of FeS in the Fe $3p \rightarrow 3d$ core-excitation region (Ref. 19). The band theoretical densities of states (DOS) for $Fe_{1/3}TiS_2$ and TiS_2 have been shifted with respect to each other prior to subtraction so that DOS structures in the S $3p$ band approximately coincide.

reproduce the satellite at $E_B=6-10$ eV. On the other hand, the experimental spectrum looks similar to the difference spectrum for FeS between the on and off resonance of the Fe $3p \rightarrow 3d$ resonant photoemission.[19] As FeS is an antiferromagnetic semiconductor with Fe^{2+} high-spin local moments,[41] its valence-band and core-level photoemission spectra are dominated by multiplet and satellite structures. Thus the similarity between the $Fe_{1/3}TiS_2$-TiS_2 difference spectrum and the on-resonance–off-resonance difference spectrum of FeS strongly suggests that the Fe $3d$ electrons in $Fe_{1/3}TiS_2$ are almost localized at least on the energy or time scale of photoemission spectroscopy due to large U, probably of the order of 5 eV.

The $Co_{1/4}TiS_2$-TiS_2 difference XPS spectrum does not show a prominent satellite in the region $E_B=6-10$ eV, unlike in the other intercalation compounds studied here. Instead, the spectrum shows a tail extending from $E_B \sim 2$ eV to ~ 8 eV accompanying the main Co $3d$ band at $E_B=0-2$ eV. We have shown in Sec. III A that the satellites in the Co $2p$ core-level XPS spectra are weak and show only tails extending on the high-binding-energy side of the main peaks. The absence of a well-defined satellite feature in both the valence-band and core-level XPS spectra would be associated with the low-spin configuration of the Co ion in the ground state, although so far no theoretical studies have been performed on the satellite structures of low-spin Co compounds.

We have shown that the intra-atomic Coulomb and multiplet-splitting (i.e., exchange) energies for the intercalated M $3d$ electrons are so large that the

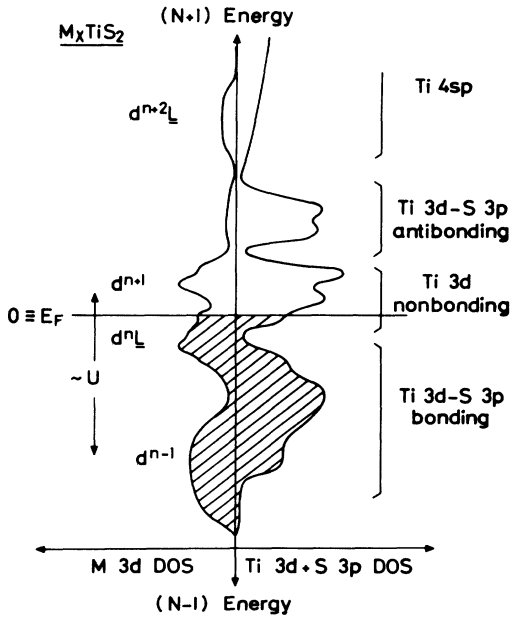

FIG. 16. Schematic representation of the spectral density of states above and below the Fermi level (E_F) for M_xTiS_2. The one-electron bandlike Ti $3d$- and S $3p$-derived states and the essentially localized M $3d$ states are hybridized with each other. The M $3d$ components at E_F may be responsible for the non-rigid-band behavior or the itinerant behavior of the M $3d$ states.

M $3d$-derived valence-band spectra cannot be described by DOS given by the itinerant-band model with one-electron approximation. The localized M $3d$ states and the bandlike Ti $3d$-S $3p$ states are strongly hybridized with each other, leading to the satellite structures in the XPS spectra, as schematically shown in Fig. 16.

We have analyzed the M $3d$-derived XPS spectra using the cluster model by implicitly assuming that the guest-atom concentration x in $M_x TiS_2$ affects solely the overall intensities of the difference spectra but not their shapes. That is, in the cluster-model analyses we have neglected interactions between guest atoms mediated by the M $3d$-S $3sp$ or M $3d$-Ti $3d$ conduction-band hybridization nor the M $3d$-Ti $3d$ conduction-band hybridization itself. The satisfactory agreement between theory and experiment suggests the validity of these approximations. However, this does not necessarily imply that these interactions are negligible for the low-energy (magnetic, electric, thermal, etc.) properties, since these interactions are effective on a smaller energy scale (10^{-4}–0.1 eV) than the energy resolution of x-ray-photoemission spectroscopy ($\sim$1 eV). The synchrotron-radiation photoemission studies with higher-energy resolution ($\sim$0.3 eV) than XPS have indeed revealed complex changes in the Ti $3d$ conduction band near E_F as a function of x for $Co_x TiS_2$,[12,13] indicating the importance of the M $3d$-Ti $3d$ conduction-band hybridization or possibly the M $3d$ intersite interaction already on the scale of $\sim$0.3 eV.

D. Auger-electron spectra

The kinetic energy of a core-valence-valence (CVV) Auger electron is given by

$$E_{\rm kin}^{A}=E_B(c)-2E_B(v)-U\ , \qquad (3)$$

where $E_B(c)$ and $E_B(v)$ denote the binding energies of the core and valence electrons. Thus one would expect to evaluate the U value for the intercalated $3d$ electrons from the $L_{2,3}M_{4,5}M_{4,5}$ ($2p$-$3d$-$3d$) Auger spectra shown in Fig. 17. However, by using the binding energy of the main M $3d$ band for $E_B(v)$ and the kinetic energy of the Auger peak for $E_{\rm kin}^{A}$ in Eq. (3), we obtain U values of about 6, 3, 1, and 0 eV, respectively, for the intercalated Ni, Co, Fe, and Mn $3d$ electrons, which, except for Ni, are too small as compared to those estimated from the analyses of the XPS spectra. This would be because the above estimate of U using Eq. (3) does not properly take into account the screening process for the valence $3d$ holes in the final states of photoemission and Auger-electron spectroscopy. While it is now established that the M $3d$ hole for the main d band is screened by transfer of one electron from the ligand S $3p$ orbital, it is not known at present what types of screening process take place in the Auger final state as well as in the Auger initial state. It has been argued that the final state of the CVV Auger transition in Fe_2O_3 is screened by transfer of two electrons from the O $2p$ to Fe $3d$ states, resulting in $d^5\underline{L}^2$ final states.[42] If this is the case for $M_x TiS_2$, the U values estimated above would be much reduced from the U values estimated from XPS. Only in the case of $Ni_{1/3}TiS_2$, the above estimate has given a U value which is consistent with that derived from the XPS spectra. As the energy position and the shape of the present Ni Auger spectrum is quite similar to those of Ni metal, for which the prominent Auger peak has been unambiguously assigned to a multiplet component of the localized $3d^8$ final state,[43] we may attribute the peak in the Ni Auger spectrum to a $3d^8$ (or $3d^8\underline{L}$ or $3d^8\underline{L}^2$) final state. The shoulder at $\sim$3 eV below $E_F(2p_{3/2})$, on the other hand, would be assigned to final states with virtually noninteracting two holes in the main d band as in Ni metal.[43] We thus suspect that the sharp difference in the $L_3M_{4,5}M_{4,5}$ Auger spectra between Ni_xTiS_2 and the other intercalation compounds is due to a rapid decrease in the intensity of the localized two-hole final states relative to that of the delocalized, virtually noninteracting two-hole states as one goes from Ni to lighter transition-metal elements. The problem of screening processes in the

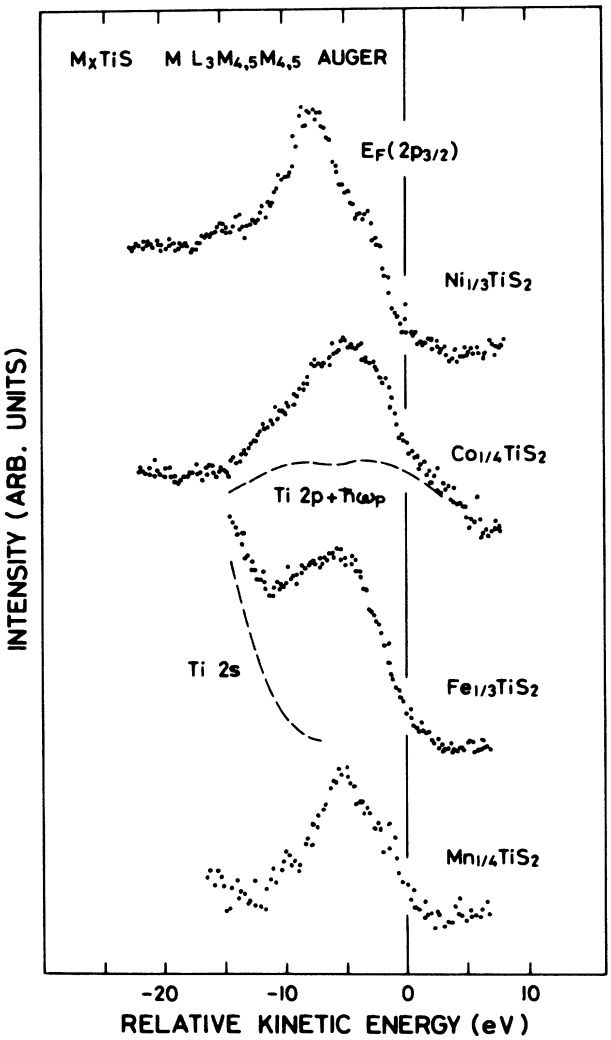

FIG. 17. $L_3M_{4,5}M_{4,5}$ Auger-electron spectra of guest $3d$ transition-metal atoms in M_xTiS_2. Kinetic energies are referenced to that equal to the M $2p_{3/2}$ core-level binding energy denoted by $E_F(\underline{2p}_{3/2})$, which correspond to a final state with two holes at the Fermi level.

Auger-electron spectroscopy of $3d$ transition-metal compounds would be an important subject which deserves further systematic investigations.

Core-core-valence (CCV) Auger-electron spectra can give local DOS on the core-hole site. The $L_{2,3}M_{2,3}M_{4,5}$ ($2p$-$3p$-$3d$) Auger-electron spectra of the guest atoms, however, show a strong multiplet effect in the final state[44] and cannot be used to study the local DOS of the ground state. As the multiplet effect is expected to be small for Ti,[45] the Ti $L_3M_{2,3}M_{4,5}$ spectrum of TiS_2 is compared with the band-theoretical Ti $3d$ partial DOS (Ref. 10) in Fig. 18. The theoretical DOS has been convoluted with the Lorentzian width of the Ti $2p$ core-level XPS spectrum plus that of Ti $3p$, and the effect of the spin-orbit splitting of the Ti $3p$ core level has also been included. [The theoretical spectrum thus obtained has been shifted to lower kinetic energies by 1 eV as we did when comparing band theory and experiment for the valence-band XPS (Sec. III C, Fig. 12).] The calculated result shown in Fig. 18 reproduces the experimental peak at the kinetic energy of $E_{kin}\sim 417$ eV, but gives no feature corresponding to the structure at $E_{kin}\sim 421$ eV. Since CCV Auger spectra give local DOS In the presence of a core hole rather than that of the ground state, we attribute the latter additional feature to an effect of the core hole. In Sec. III B, we have argued that a Ti $3d$-like screening orbital is formed below E_F in the core-hole state but in the case of TiS_2 cannot be immediately filled in the sudden process of the core-level photoemission. We suspect that, in the initial state of the $L_3M_{2,3}M_{4,5}$ Auger transition, the screening orbital is filled by an electron prior to the Auger transition through the other Auger-type process discussed in Sec. III B which fills the screening level and leaves two holes in the Ti $3d$ conduction band. As the additional feature at $E_{kin}\sim 421$ eV corresponds energetically to Ti $3d$-like states near E_F [$E_F(2p_{3/2}\underline{3p})$ in Fig. 18], we attribute the 421-eV feature to the screening level which is filled in the Auger initial state. This assignment is consistent with the increase in the Auger emission intensity at $E_{kin}\sim 421$ eV on going from TiS_2 to M_xTiS_2 as shown in Fig. 19, since the Ti $3d$ conduction band is par-

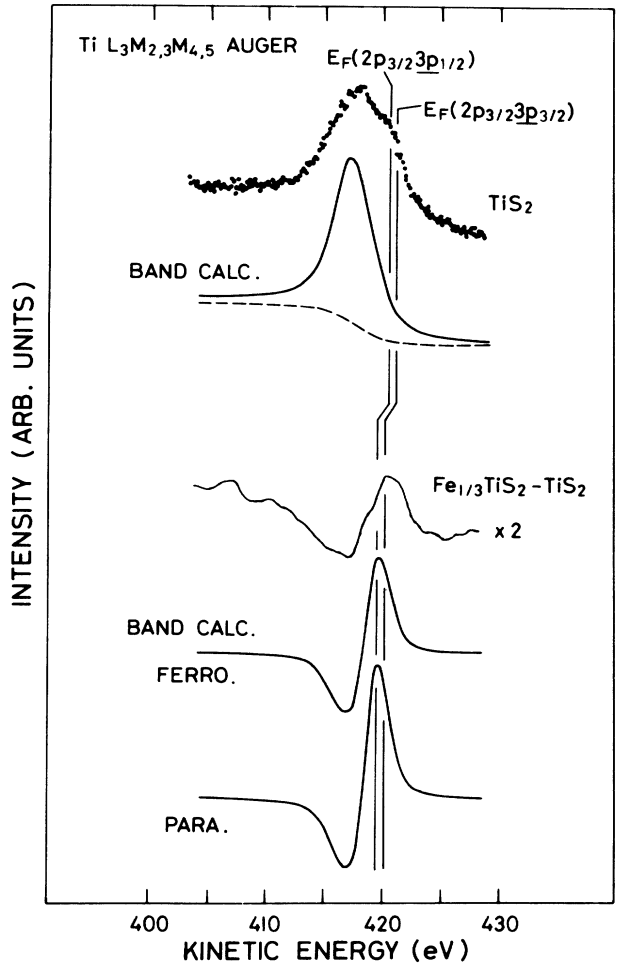

FIG. 18. Comparison of the Ti $L_3M_{2,3}M_{4,5}$ Auger-electron spectra with the Ti $3d$ partial densities of states (DOS) given by band-structure calculations on TiS_2 (Ref. 10) and $Fe_{1/3}TiS_2$ (Ref. 11). The raw data for TiS_2 and the $Fe_{1/3}TiS_2$-TiS_2 difference spectrum are compared with the band theory. $E_F(2p_{3/2}\underline{3p}_{1/2})$ and $E_F(2p_{3/2}\underline{3p}_{3/2})$ mark kinetic energies equal, respectively, to $E_B(2p_{3/2})-E_B(3p_{1/2})$ and $E_B(2p_{3/2})-E_B(3p_{3/2})$, corresponding to the Fermi level of the valence ($M_{4,5}$) electrons.

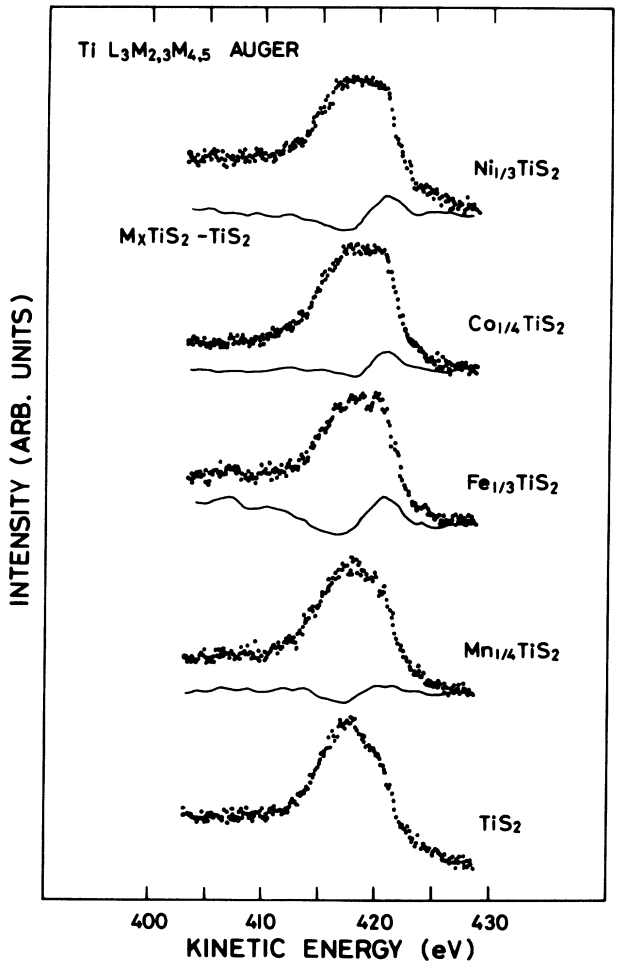

FIG. 19. Ti $L_3M_{2,3}M_{4,5}$ Auger-electron spectra of TiS_2 and M_xTiS_2. Difference spectra between M_xTiS_2 and TiS_2 are shown by solid curves below each of the M_xTiS_2 spectra.

tially filled already in the ground state of the intercalation compounds.

In Fig. 19 one can see that the 417-eV feature becomes weaker by intercalation, while the 421-eV feature becomes more intense. In order to clarify these changes, difference spectra between M_xTiS_2 and TiS_2 are obtained by normalizing and shifting the spectra so that the Ti $L_3M_{2,3}M_{2,3}$ ($2p_{3/2}$-$3p$-$3p$) spectra are cancelled out and are shown by solid curves in the same figure. As we have assigned the 417-eV feature to the Ti $3d$ component hybridized in the S $3p$ band and the 421-eV feature to the partially filled Ti $3d$ conduction band (in the ground state or the core-hole state), the decrease in the intensity of the 417-eV peak with intercalation suggests that the Ti $3d$—S $3p$ bonding is weakened through the formation of the M $3d$—S $3p$ bond. If we assume that the contributions of the screening level to the intensity of the 421-eV feature are of the same magnitude for TiS_2 and M_xTiS_2, then these contributions would be canceled out in the difference Auger spectra and the difference spectra would represent changes in the Ti $3d$ DOS in the ground state induced by the intercalation. Then we expect good correspondence between band theory and experiment for the $M_xTiS_2-TiS_2$ difference spectra if band theory is relevant to the Ti $3d$-like states. Indeed, as shown in Fig. 18, we find good agreement between the band theory[10,11] and experiment for the $Fe_{1/3}TiS_2$-TiS_2 difference Auger-electron spectrum.

IV. CONCLUSIONS

We have studied the electronic structure of intercalation compounds M_xTiS_2 (M=Mn, Fe, Co, and Ni) by using x-ray-photoemission and Auger-electron spectroscopy. From the multiplet and satellite structures in the M $3d$-derived XPS spectra in the valence-band region as well as in the M $2p$ core-level XPS and the M $L_3M_{4,5}M_{4,5}$ Auger-electron spectra, we conclude that the intra-atomic Coulomb and exchange energies for the intercalated $3d$ electrons and the M $3d$-S $3p$ hybridization strength are greater than the M $3d$ one-electron bandwidth. On the other hand, the valence-band, core-level, and Auger-electron spectra involving Ti and S states indicate that electron correlation is not important for Ti $3d$- and S $3p$-derived states, giving support to the one-electron energy-band description for the host Ti $3d$- and S $3p$-derived states as in many Ti and S compounds. While the magnetic orderings appear to be largely determined by the superexchange and RKKY interactions between the localized M $3d$ magnetic moments as in the rigid-band model, the itinerant-band model including the M $3d$ electrons seems to explain some of the magnetic, thermal, and transport (low-energy) properties.[7-9] In the light of the present photoemission results, these two conflicting descriptions of the electronic structure may be reconciled with each other by considering a formation of correlated $3d$ bands as a result of hybridization between the essentially localized M $3d$ and the bandlike host Ti $3d$-S $3p$ states.

The formation of correlated $3d$ bands as a result of hybridization between the localized $3d$ and bandlike states is a general feature of late $3d$ transition-metal compounds as has recently been pointed out for NiS and related sulfides.[46,47] The band gaps in insulating compounds of late $3d$ transition metals (Fe, Co, Ni, and Cu) are of the $d^n\underline{L}-d^{n+1}$ type, namely the gaps are formed between the unoccupied d and occupied ligand p states. In metallic compounds such as NiS, these gaps are closed due to the relatively high nonmetal p band and/or the low unoccupied $3d$ states.[47,48] In the case of M_xTiS_2, the gap is already closed in the host semimetallic TiS_2, and therefore the intercalated $3d$ states will acquire itinerant character through hybridization with electronic states near E_F irrespective of the S $3p$ and M $3d$ energy positions, although the degree of itinerancy will depend on the energy positions of the S $3p$ and M $3d$ states. Interactions among the guest atoms which are important in determining the low-energy transport properties and magnetic orderings could not be identified in the present study. However, we note that the intersite interactions mediated by the S $3p$ band are second-order processes with respect to the M $3d$-S $3p$ hybridization evaluated in the present work and can in principle be studied by extending the cluster model to the periodic Anderson Hamiltonian.[49]

ACKNOWLEDGMENTS

We would like to thank Professor N. Suzuki for sending us reports of their work prior to publication. FeS samples were supplied by Dr. H. Wada and NiS samples by Mr. M. Matoba and Professor S. Anzai.

*Present address: Department of Physics, The University of Tokyo, Tokyo 113, Japan.

[1]G. V. Subba and M. W. Shafer, in *Intercalated Layered Materials*, edited by F. Levy (Reidel, Dordrecht, 1976), p. 423.

[2]R. H. Friend and A. D. Yoffe, Adv. Phys. **36**, 1 (1987).

[3]T. Miyadai, K. Kikuchi, H. Kondo, S. Sakka, M. Arai, and Y. Ishikawa, J. Phys. Soc. Jpn. **52**, 1394 (1983).

[4]R. H. Friend, A. R. Beal, and A. Yoffe, Philos. Mag. **35**, 1269 (1980).

[5]S. S. P. Parkin and R. H. Friend, Philos. Mag. **41**, 65 (1980); **41**, 95 (1980).

[6]S. S. P. Parkin, E. A. Marseglia, and P. J. Broun, J. Phys. C **16**, 2749 (1983).

[7]H. Negishi, A. Shoube, H. Takahashi, Y. Ueda, M. Sasaki, and M. Inoue, J. Magn. Magn. Mater. **67**, 179 (1987); M. Inoue, M. Matsumoto, H. Negishi, and H. Sakai, *ibid.* **53**, 131

(1985).
[8]M. Inoue, Y. Muneta, H. Negishi, and M. Sasaki, J. Low Temp. Phys. **63**, 235 (1986).
[9]M. Koyano, H. Negishi, Y. Ueda, M. Sasaki, and M. Inoue, Solid State Commun. **62**, 261 (1987).
[10]T. Yamasaki, N. Suzuki, and K. Motizuki, J. Phys. C **20**, 419 (1987).
[11]N. Suzuki, T. Yamasaki, and K. Motizuki, J. Magn. Magn. Mater. **20**, 64 (1987).
[12]Y. Ueda, H. Negishi, M. Kotano, M. Inoue, K. Soda, H. Sakamoto, and S. Suga, Solid State Commun. **57**, 839 (1986).
[13]Y. Ueda, K. Fukushima, H. Negishi, M. Inoue, M. Taniguchi, and S. Suga, J. Phys. Soc. Jpn. **56**, 2471 (1987).
[14]M. Inoue and H. Negishi, J. Phys. Soc. Jpn. **54**, 380 (1985).
[15]P. W. Palmberg, J. Electron Spectrosc. Relat. Phenom. **5**, 691 (1974).
[16]D. K. G. de Boer, C. Haas, and G. A. Sawatzky, Phys. Rev. B **29**, 4401 (1984).
[17]See, e.g., L. C. Davis, J. Appl. Phys. **59**, R25 (1986).
[18]H. van der Heide, R. Hemmel, C. F. van Bruggen, and C. Haas, J. Solid State Chem. **33**, 17 (1980).
[19]A. Fujimori, H. Wada, M. Taniguchi, and S. Suga (unpublished).
[20]S. Hüfner, T. Riesterer, and F. Hulliger, Solid State Commun. **54**, 689 (1985).
[21]The hexagonal form of NiS is antiferromagnetic below ~ 260 K with an ordered moment of $\sim 1.7\mu_B$ and is Pauli paramagnetic above ~ 260 K [J. T. Sparks and T. Komoto, Phys. Lett. **25A**, 398 (1967); S. Anzai and K. Ozawa, J. Phys. Soc. Jpn. **24**, 271 (1968)]. However, the photoemission spectra do not change appreciably between the two phases and show characteristic features of the high-spin divalent ground state [A. Fujimori, K. Terakura, M. Taniguchi, S. Ogawa, S. Suga, M. Matoba, and S. Anzai, Phys. Rev. B **37**, 3109 (1988)].
[22]T. Riesterer, L. Schlapbach, and S. Hüfner, Solid State Commun. **57**, 109 (1986).
[23]S. P. Friedman and V. A. Gubanov, Zg. Neorg. Khim. **30**, 2501 (1985) [Russ. J. Inorg. Chem. **30**, 1424 (1985)].
[24]D. A. Shirley, in *Photoemission in Solids I,* edited by M. Cardona and L. Ley (Springer-Verlag, Berlin, 1978), p. 165.
[25]B. M. Veal and A. P. Paulikas, Phys. Rev. Lett. **51**, 1995 (1983).
[26]T. Miller and T.-C. Chiang, Phys. Rev. B **29**, 1121 (1984).
[27]C. S. Fadley, D. A. Shirley, A. J. Freeman, P. S. Bagus, and J. V. Mallow, Phys. Rev. Lett. **23**, 1397 (1969).
[28]S. Doniach and M. Šunjić, J. Phys. **3**, 285 (1970).
[29]G. D. Mahan, Phys. Rev. B **11**, 4814 (1975). We have employed this line shape rather than that of Ref. 28. However, as ζ in $I(E) \propto {}^{-E/\zeta}/E^{1-\alpha}$ has been fixed sufficiently large, 9 eV, the line shape is almost the same as that of Ref. 28.
[30]The spin-orbit splitting ΔE_{so}, and the Loretnzian full width at half maximum (FWHM), 2γ, for $M_x TiS_2$ were fixed to the same values as those of TiS_2. This was done because the lifetime of the S $2p$ core hole which is largely determined by the $L_{2,3}VV$ Auger transitions (V denotes the S $3sp$ electron) would not be significantly different between TiS_2 and $M_x TiS_2$ since the number of S $3sp$ electrons would be nearly the same.
[31]M. Koyano, H. Negishi, Y. Ueda, M. Sasaki, and M. Inoue, Phys. Status Solidi B **138**, 357 (1986).
[32]G. K. Werthiem and P. H. Citrin, *Photoemission in Solids I,* Ref. 24, p. 197.
[33]The lifetime width of the $2p_{1/2}$ peak is larger than that of $2p_{3/2}$ owing to the L_2L_3V Coster-Kronig decay of the $2p_{1/2}$ core hole, where V denotes a valence electron. This decay process transforms most of the $2p_{1/2}$ holes into $2p_{3/2}$ ones before they decay via L_2MM Auger process, thereby making the L_2MM Auger-electron emission intensity much smaller than the L_3MM intensity. The same is true for the $L_{2,3}MM$ Auger-electron spectra of the guest $3d$ atoms.
[34]A. Kotani and Y. Toyozawa, J. Phys. Soc. Jpn. **37**, 912 (1974).
[35]As the number of parameters is large in this model, we have made the following constraints in order to achieve numerical convergence. The Lorentzian widths of the $2p_{3/2}$ well-screened peaks, $2\gamma_{3/2}$, have been fixed at the value for TiS_2; the additional lifetime broadening of the $2p_{1/2}$ peak with respect to $2p_{3/2}$, i.e., $2\gamma_{1/2}-2\gamma_{3/2}$, due to the L_2L_3V Coster-Kronig process has been assumed to be the same for the well-screened and poorly screened peaks; the Gaussian width has been fixed at the value for TiS_2; the α of the poorly screened peaks has been set to zero (Ref. 34). Multiplet effects may be present for the well-screened peaks since the peaks correspond to final states with an electron in the Ti $3d$-like screening orbital. Indeed, the $2\gamma_{3/2}$ values assumed for $M_x TiS_2$ are consistent with the multiplet broadening, as the lifetime width of the $2p_{3/2}$ XPS peak for Ti metal has been found broader than the theoretical one by ~ 0.5 eV [J. C. Fuggle and S. F. Alvaredo, Phys. Rev. B **22**, 1615 (1980)] due to the multiplet effect. No multiplet effect is expected for the Ti $2p_{3/2}$ XPS peak of TiS_2 since there is no screening electron, but the peak is expected to be lifetime broadened as it decays into a well-screened core-hole state (see the next paragraphs in the text). The large $2\gamma_{3/2}$ value of ~ 0.9 eV for TiS_2 (Table II) would be due to this lifetime-broadening effect, as it has been calculated to be ~ 0.2 eV for the free Ti atom [M. O. Krause, J. Phys. Chem. Ref. Data **8**, 307 (1979)].
[36]J. Zaanen, C. Westra, and G. A. Sawatzky, Phys. Rev. B **33**, 8060 (1986).
[37]J. H. Scofield, J. Electron Spectrosc. Relat. Phenom. **8**, 129 (1976).
[38]A. Fujimori, K. Terakura, M. Taniguchi, S. Ogawa, S. Suga, M. Matoba, and S. Anzai, Ref. 21; J. Magn. Magn. Mater. **70**, 67 (1987), and unpublished results.
[39]Possible changes in the host Ti $3d$—S $3p$ bonding band induced by intercalation have been neglected, as they are expected to be relatively small and are difficult to separate out from the difference spectra. In fact, changes in the Ti $3d$ component in this band are found to be small from the Ti $L_3M_{2,3}M_{4,5}$ Auger spectra (Sec. III D).
[40]P. S. Bagus, C. R. Brundle, T. J. Chuang, and K. Wandelt, Phys. rev. Lett. **39**, 1229 (1977).
[41]M. J. D. Coey, H. Roux-Buisson, and R. Brusetti, J. Phys. (Paris) Colloq. **37**, C4-1 (1976).
[42]A. Fujimori, M. Saeki, N. Kimizuka, M. Taniguchi, and S. Suga, Phys. Rev. B **34**, 7318 (1986).
[43]N. Mårtensson, R. Nyholm, and B. Johansson, Phys. Rev. **30**, 2245 (1984).
[44]J. F. McGilp and P. Weightman, J. Phys. C **11**, 643 (1978).
[45]T. Yamaguchi, S. Shibuya, and S. Sugano, J. Phys. C **15**, 2625 (1982).
[46]J. Zaanen, G. A. Sawatzky, and J. W. Allen, Phys. Rev. Lett. **55**, 418 (1985); S. Hüfner, Z. Phys. B **61**, 135 (1985).
[47]S. Hüfner, Z. Phys. B **58**, 1 (1984).
[48]A. Fujimori, in *Core-Level Spectroscopy in Condensed Systems, Springer Series in Solid-State Sciences,* edited by J. Kanamori and A. Kotani (Springer-Verlag, Berlin, 1988).
[49]J. W. Allen, J. Magn. Magn. Mater. **47-48**, 168 (1985).